Reduction of ferrihydrite with adsorbed and coprecipitated organic matter: Microbial reduction by *Geobacter bremensis* versus abiotic reduction by Na-dithionite

K. Eusterhues[1], A. Hädrich[2], J. Neidhardt[1], K. Küsel[2,3], T. F. Keller[4,*], K. D. Jandt[4], K. U. Totsche[1]

[1]{Institut für Geowissenschaften, Friedrich-Schiller-Universität Jena, 07749 Jena, Germany}

[2]{Institut für Ökologie, Friedrich-Schiller-Universität Jena, 07743 Jena, Germany}

[3]{German Centre for Integrative Biodiversity Research (iDiv) Halle-Jena-Leipzig, 04103 Leipzig, Germany}

[4]{Chair of Materials Science, Otto Schott Institute of Materials Research, Faculty of Physics and Astronomy, Friedrich-Schiller-University Jena, 07743 Jena, Germany}

[*]{now at: Deutsches Elektronen-Synchrotron DESY, 22607 Hamburg, Germany}

Correspondence to: K. Eusterhues (karin.eusterhues@uni-jena.de)

Abstract

Ferrihydrite is a widespread poorly crystalline Fe oxide which becomes easily coated by natural organic matter in the environment. This mineral-bound organic matter entirely changes the mineral surface properties and therefore the reactivity of the original mineral. Here, we investigated 2-line ferrihydrite, ferrihydrite with adsorbed organic matter, and ferrihydrite co-precipitated with organic matter for microbial and abiotic reduction of Fe(III). Ferrihydrite-organic matter associations with different organic matter-loadings were reduced either by *Geobacter bremensis* or abiotically by Na-dithionite. Both types of experiments showed decreasing initial Fe reduction rates and decreasing degrees of reduction with increasing amounts of mineral-bound organic matter. At similar organic matter-loadings, coprecipitated ferrihydrites were more reactive than ferrihydrites with adsorbed organic matter. The difference can be explained by the smaller crystal size and poor crystallinity of such coprecipitates. At small organic matter loadings the poor crystallinity of coprecipitates led to even faster Fe reduction rates than found for pure ferrihydrite. The amount of mineral-bound organic matter also affected the formation of secondary minerals: goethite was only

found after reduction of organic matter-free ferrihydrite and siderite was only detected when ferrihydrites with relatively low amounts of mineral-bound organic matter were reduced. We conclude that direct contact of *G. bremensis* to the Fe oxide mineral surface was inhibited by attached organic matter. Consequently, mineral-bound organic matter shall be taken into account as a factor in slowing down reductive dissolution.

1 Introduction

Natural Fe oxides are typically nanoparticles and contribute significantly to the total surface area and reactivity of a soil (Karltun et al., 2000; van der Zee et al., 2003; Eusterhues et al., 2005; Regelink et al., 2013). Due to their high reactivity towards dissolved organic matter (Torn et al., 1997; Kaiser and Zech 2000) Fe oxides are partially or completely covered by organic matter in natural environments. Organic coverage may result in surfaces properties strongly different from those of the original oxides, with consequences for aggregation, mobility, and solubility.

One of the most common Fe oxides is poorly crystalline ferrihydrite, usually forming aggregates of nanometer-sized individual crystals (Jambor and Dutrizac, 1998; Bigham et al., 2002; Cornell and Schwertmann, 2003). In contrast to adsorption of organic matter on pre-existing ferrihydrite surfaces, coprecipitation leads to adsorption and occlusion (physical entrapment) of organic molecules in the interstices between the ferrihydrite crystals. Additionally, the presence of dissolved organic matter inhibits ferrihydrite growth (Schwertmann et al., 2005; Mikutta et al., 2008; Eusterhues et al., 2008; Cismasu et al., 2011), and so coprecipitated ferrihydrites tend to develop smaller crystal sizes and more crystallographic defects. Likewise, the aggregation behavior of ferrihydrites may be affected. Since ferrihydrite is often formed in organic matter-rich solutions, e.g., in sediments and soils, we assume that coprecipitation is a common process in nature. As coprecipitated ferrihydrites differ in many properties from pure ferrihydrites, we suppose that the accessibility and solubility of ferrihydrite surfaces as well as the accessibility of the adsorbed/occluded organic matter to microorganisms, extracellular enzymes, redox active shuttling compounds or reducing agents may differ from ferrihydrites with purely adsorbed organic matter.

In the past, dissolved humic acids from alkaline extracts have been added to microbial experiments to test their influence on ferric iron reduction. It was suggested that they may enhance Fe(III) reduction by electron shuttling (Lovley et al., 1996; Hansel et al., 2004; Jiang and Kappler, 2008; Roden et al., 2010), complexation of Fe(II) (Royer et al., 2002) or

complexation and dissolution of Fe(III) (Jones et al., 2009). Amstaetter et al. (2012) and Jiang and Kappler (2008) observed that the concentration of humic acid or the mineral/humic acid ratio may control whether humic acids increase reduction or not. At high Fh concentrations in solution (30mM), Amstaetter et al. (2012) even observed a decrease in Fe(III) reduction due to humic acid addition. The decrease was explained by an increased aggregation and a therefore reduced accessibility of the Fe oxide surface for bacteria. The influence of mineral-bound organic matter on reduction and mineral transformation is less well investigated. We are aware of only three articles: Henneberry et al. (2012) coprecipitated ferrihydrite with dissolved organic matter from an agricultural drain and exposed the products to S(-II) and Fe(II). Neither a release of the mineral-associated organic matter nor a mineral transformation was observed during reduction. Pédrot et al. (2011) produced nanometer-sized lepidocrocite and Fe-humic acid coprecipitates and compared its reduction by *Shewanella putrefaciens*. They found the reduction of the coprecipitates to be about eight times faster than that of pure lepidocrocite. Shimizu et al. (2013) studied the influence of coprecipitated humic acid on ferrihydrite reduction by *Shewanella putrefaciens* strain CN32. Low C/Fe ratios were reported to decrease the reduction of the ferrihydrite-humic acid associations, whereas an increased reactivity was found at high C/Fe ratios. In addition, the mineral-bound humic acid changed the mineral transformation during reduction. The formation of goethite was inhibited, the formation of magnetite decreased and the formation of a green rust-like phase stimulated (Shimizu et al., 2013). Such changes in the mineral assemblage will strongly affect the cycling of Fe.

Our study aims to enlighten changes in microbial and abiotic Fe(III) reduction caused by mineral-bound organic matter. A water extract of a Podzol forest floor was used as organic matter and served to represent dissolved soil organic matter. We produced ferrihydrites with different organic matter loadings by adsorption and coprecipitation, which were then exposed to microbial reduction by *Geobacter bremensis* and chemical reduction by Na-dithionite. *Geobacter bremensis* is common in soil and serves as a well investigated model organism for dissimilatory Fe(III) reduction. Main objectives were to find out whether mineral-bound organic matter increases or decreases ferrihydrite reactivity and whether coprecipitates differ in reactivity from ferrihydrites with adsorbed organic matter. The formation of secondary minerals was followed by XRD.

2 Methods

2.1 Materials

All chemicals used in this study were reagent grade. For preparation of stock solution and media, 18 MΩ doubly deionized water was used. *Geobacter bremensis* (DSM 12179; Straub & Buchholz-Cleven, 2001) was obtained from the German Resource Centre for Biological Material (DSMZ, Braunschweig).

2.2 Extraction of soil organic matter

A forest floor extract was obtained from the Oa and Oe layers of a Podzol under spruce close to Freising, Germany. These layers represent the fermented and humified organic horizons below the fresh plant litter, but above the mineral soil. The Forest floor samples were air-dried and passed through a 2-mm sieve to remove coarse plant remnants. Aliquots of 150 g soil and 700 ml deionized H_2O were shaken end-over-end for 16 hours at room temperature and then centrifuged. The supernatant was pressure-filtered through polyvinylidene fluoride (Durapore; 0.45 µm pore width) membranes, concentrated in low temperature rotary evaporators and freeze-dried. The C and N concentration of the forest floor extract was measured using a CN analyzer (Vario EL, Elementar Analysensysteme, Hanau, Germany). A transmission FTIR spectrum was collected using the Nicolet iS10 (Thermo Fisher Scientific, Dreieich, Germany; see below). A solid-state ^{13}C NMR spectrum was acquired with a Bruker DSX-200 NMR spectrometer (Bruker BioSpin, Karlsruhe, Germany), applying cross polarization with magic angle spinning (CP MAS) at a spinning frequency of 6.8 kHz and a contact time of 1 ms. A ramped ^{1}H pulse was used during contact time to circumvent spin modulation of Hartmann-Hahn conditions. Pulse delays between 200 and 2000 ms were chosen.

2.3 Synthesis of ferrihydrite and ferrihydrite-organic matter associations

Two-line ferrihydrite was produced by titrating a 0.01 M $Fe(NO_3)_3$ solution with 0.1 M NaOH to pH 5 under vigorous stirring. A series of ferrihydrites with different amounts of adsorbed organic matter were produced by mixing forest floor extract solutions of different C concentrations with suspensions of freshly precipitated 2-line ferrihydrite at pH 5. The molar C/Fe ratio of the initial solutions was AFhA 0.4, AFhB 1.3, and AFhD 4.2. Coprecipitated ferrihydrites were obtained by dissolving $Fe(NO_3)_3$ in forest floor extract solutions of different concentrations and adding 0.1 M NaOH under vigorous stirring until a pH of 5 was reached. The molar C/Fe ratio of these initial solutions was CFhA 0.4, CFhB 1.3, and CFhD 4.2. The solid/solution (g/L) ratio varied between 0.3 and 1.6 for all syntheses. The solid products were separated by centrifugation, washed twice with deionized H_2O and freeze-dried. The C concentration of these samples was analyzed with the CN analyzer (Vario EL,

Elementar Analysensysteme, Hanau, Germany). Transmission FTIR spectra were taken (Nicolet iS10, Thermo Fisher Scientific, Dreieich, Germany) on pellets of 2 mg sample diluted with 200 mg KBr between 4000 and 400 cm^{-1}, accumulating 32 scans at a resolution of 4 cm^{-1}. The spectra were baseline corrected by subtracting a straight line running between the two minima of each spectrum and normalized by dividing each data point by the spectrums maximum. The second derivative was calculated using the Savitzky-Golay algorithm over 19-23 points. The specific surface area of the pure ferrihydrite was measured by N_2 gas adsorption (Autosorb1, Quantachrome, Odelzhausen, Germany) and calculated according to the BET- equation from 11 data points in the relative pressure range of 0.05 to 0.3. Prior to the measurements the sample was outgassed for at least 16 hours at 343 K in vacuum to remove adsorbed water from the sample surfaces. X-ray photoelectron spectra (XPS) were recorded using a Quantum 2000 (PHI Co., Chanhassen, MN, USA) instrument with a focused monochromatic $Al_{K\alpha}$ source (1486.7 eV) for excitation. For the high resolution spectra, the pass energy was set to 58.70 eV. After subtracting a Shirley-type background, P2p and N1s spectra were evaluated by fitting single pseudo-Voigt profiles (Lorentz portion = 0.2) to the measured data. Fe2p spectra were fitted by a pre-peak, a surface peak, and four multiplet peaks of decreasing intensity as proposed by McIntyre and Zetaruk (1977) and Grosvenor et al. (2004) for high spin Fe(III) compounds. Distances between multiplets were constrained to 1 eV, the FWHM was set to 1.4 eV and the Lorentz portion of the pseudo-Voigt curves was 0.2. The C1s peak was fitted using four pseudo-Voigt profiles with a fixed FWHM of 1.9 and a Lorentz portion of 0.2. The distances between the peaks were fixed to 1.6, 1.6, and 1.1 eV from lower to higher binding energies to distinguish the C1s binding states C-C, C-H, C-O, C-N, C=O, N-C=O and O-C=O.

2.4 Microbial reduction experiments

Differences in reducibility of ferrihydrite and ferrihydrite-organic matter associations and secondary mineralization were studied in liquid cultures inoculated with *G. bremensis*. A defined freshwater medium based on the *Geobacter* medium ATCC 1957, containing 1.5 g L^{-1} NH_4Cl and 0.1 g L^{-1} KCl was used. After autoclaving and cooling under an N_2/CO_2 (80/20 v/v) atmosphere, 30 ml L^{-1} of 1 M $NaHCO_3$ (autoclaved, CO_2), 10 ml L^{-1} Wolfe's vitamin solution (ATCC 1957), 10 ml L^{-1} modified Wolfe's minerals (ATCC 1957) and sodium-acetate (7 mM) as carbon source were added. Unless stated otherwise, added solutions were prepared under anoxic (N_2) conditions and filter sterilized (0.2 µm, PVDF). NaH_2PO_4 from the original recipe was not added to avoid interaction of PO_4^{3-} with ferrihydrite. The final

medium had a pH of 6.8. The pH was chosen because recommended for optimum growth of *Geobacter*, by both the DSMZ (Medium 579, pH 6.7 to 7.0) as well as the ATCC (Medium 1957, pH 6.8). Adsorption and coprecipitation experiments were performed at pH 5, i.e. under pH conditions where most coprecipitates form in the presence of dissolved organic matter (Eusterhues et al., 2011). However, the higher pH during reduction experiments may have caused desorption of some of the mineral-bound organic matter.

The medium (10 ml) was dispensed under an N_2 gas stream into pre-sterilized (6 h 180 °C) 21 ml-culture tubes that contained pre-weighed ferrihydrite and ferrihydrite-organic matter associations (40 mM per tube). After tubes were closed with butyl rubber stoppers and capped with aluminium rings, they were flushed again with sterile N_2/CO_2 (80/20 v/v), applying an overpressure of ~100 mbar. Pressure was monitored with a needle tensiometer (TensioCheck TC1066, Tensiotechnik). Inoculation of ferrihydrite and ferrihydrite-organic matter associations was performed with 4.8% (v/v; initial cell density ~10^8 mL^{-1}) *G. bremensis* pre-culture grown on phosphate-free medium with sodium-fumarate (50 mM) as electron acceptor and sodium-acetate (20 mM) as electron donor and carbon source. Triplicate samples of all treatments were incubated horizontally (30 °C) in the dark and shaken periodically.

For Fe(II) determination, 0.2 ml subsamples were taken anoxically from well shaken culture tubes with a syringe and transferred into 0.5 M HCl for extraction (1 h in the dark). Fe(II) of the extraction solutions was determined using the phenanthroline assay (Tamura et al., 1974). Fe(total) was analyzed via ICP-OES (Spectroflame, Spectro, Kleve, Germany). Solid remnants of the incubation experiments were freeze dried and stored under N_2 until XRD measurements (D8 Advance DaVinci diffractometer by Bruker AXS, Karlsruhe, Germany) were performed using Cu Kα radiation at 40 kV and 40 mA.

2.5 Abiotic reduction experiments with Na-dithionite

Chemical reducibility of ferrihydrite and ferrihydrite-organic matter associations was evaluated in abiotic reduction experiments performed after Houben (2003). In short, ferrihydrite and ferrihydrite-organic matter associations (ca. 0.1 mmol Fe in ferrihydrite) were added to 0.5 L of anoxic (N_2) 0.01 M Na-dithionite solution buffered with ca. 0.015 M $NaHCO_3$ in a 1L screw cap bottle. Bottles were closed immediately with a rubber stopper and a metal screw cab, shaken thoroughly and afterwards stirred constantly at room temperature. The solution pH was adjusted to ~7 before ferrihydrite addition by shortly purging with CO_2 and was stable during the experiment. Periodically, samples of 0.5 ml were taken with N_2 flushed syringes and filtered through 0.2 µm membranes (PVDF) into cuvettes filled with 0.5

ml acetate (to quench the reduction) and ddH_2O (for dilution). The dissolved Fe(II) was measured using the phenantroline method (Tamura et al., 1974).

2.6 Evaluation of reduction rates:

Fe(II) formation kinetics were used as analogues for Fe(III) reduction. Apparent initial reaction rates were estimated by fitting linear regression lines to Fe(II)/Fe(total) versus time for the first data points acquired in microbial and abiotic reduction experiments. The slope of the line represents the initial reaction rate. The degree of dissolution was determined at day 17 for microbial experiments and after 75 min for abiotic experiments. Day 17 for microbial experiments was chosen, because the Fe(II)/Fe(total) of the ferrihydrite control at day 52 is much lower than at day 17 and therefore probably wrong. We assume that this is due to unintentional oxidation at the end of the experiment in this sample. The data were fit also to a model proposed first by Christoffersen and Christoffersen (1976) and used successfully by e.g. Postma (1993), Larsen and Postma (2001), Houben (2003), and Roden (2004):

$$m_t / m_0 = \left[-k(1-\gamma)t+1\right]^{1/(1-\gamma)}$$

where m_0 is the initial concentration of Fe(III), m_t the concentration of Fe(II) at time t, k the rate constant, and γ a constant describing the Fe mineral reactivity as controlled by crystal size, morphology, structure and available reactive surface sites (Postma, 1993; Roden, 2004). While we were successful in fitting the abiotic variants, the model failed to reconstruct the biotic dissolution variants (data not shown). This may point to other processes involved in the biotic dissolution, e.g., a preferential selection of a size fraction of the ferrihydrite-organic matter-associations. However, the comparably poor data quality of the biotic variants does not allow for an in-depth interpretation of this finding.

3 Results and Discussion

3.1 Characterization of forest floor extract, control ferrihydrite and ferrihydrite-organic matter associations

The forest floor extract for the production of ferrihydrite-organic matter associations was characterized by its C/N ratio, solid state ^{13}C NMR (Figure 1) and FTIR (Figure 2). The concentrations of C and N were found to be 35.1% and 4.3%. Organic C in the respective chemical shift regions of the NMR spectrum was quantified to 13% of TOC alkyl C (0-45 ppm), 51% of TOC O-alkyl C (45-110 ppm), 24% of TOC aryl C (110-160 ppm), and 13% of TOC carbonyl C (160-220 ppm). In comparison to the material used for previous adsorption

and coprecipitation studies (Eusterhues et al., 2008; Eusterhues et al., 2011; Eusterhues et al., 2014) this material had a higher content in aromatic groups and carbonyl C (ester, carboxyl or amide groups), and less carbohydrates. The FTIR spectrum (Figure 2; band assignment according to Abdulla et al., 2010) shows strong peaks at 1722 cm^{-1} (C=O of COOH), 1622 cm^{-1} (complexed COO^-) and at 1148, 1089, and 1041 cm^{-1} (C-O in carbohydrates). Very sharp signals at 1384 and 825 cm^{-1} are caused by NO_3^-, and show that only part of the N can belong to amides. Additional smaller signals can be identified using the second derivative of the spectrum: the signal at 1783 cm^{-1} points to the C=O stretching of γ-lactones, signals at 1547 and 1268 cm^{-1} can be explained by amide II and amide III, signals at 1512 and 1218 cm^{-1} are in accordance with the C=C stretching of aromatic rings and with the asymmetric C-O stretching of aromatic OH. The signal at 965 cm^{-1} belongs to the O-H out of plane bending of carboxylic acids and the band at 660 cm^{-1} to the O-H out of plane bending of carbohydrates.

The control ferrihydrite as well as the ferrihydrites in coprecipitates and adsorption complexes displayed XRD patterns of a typical 2-line ferrihydrite (Cornell and Schwertmann, 2003). The specific surface area of the control ferrihydrite was 197 $m^2\ g^{-1}$ as determined by N_2 gas adsorption and the concentrations of C and N were found to be 0.2% and 1.3%. The FTIR spectrum (Figure 2) showed that this high N concentration is due to nitrate, which has not been fully removed during ferrihydrite synthesis from $Fe(NO_3)_3 \cdot 9\ H_2O$. [We assume that the nitrate contamination does not affect our microbial reduction experiments, because *Geobacter bremensis* is not able to reduce nitrate (Straub et al., 1998; Straub et al., 2001).]

The adsorption isotherm (Figure 3) can be described by a BET model (Ebadi et al., 2009) with a monolayer adsorption capacity of q_m=0.52 mg m^{-2}, an equilibrium constant of adsorption for the first layer of K_S = 0.9 L mg^{-1}, and an equilibrium constant of adsorption for further layers of K_L= 0.0045 L mg^{-1}. The obtained monolayer loading is in accordance with other adsorption studies involving natural organic matter adsorption and ferrihydrite (Tipping et al., 1981; Kaiser et al. 2007; Eusterhues et al., 2005). Coprecipitation, in contrast, produced considerably larger organic matter-loadings of ~1.1 mg m^{-2}. This can be explained either by a larger surface area of coprecipitated ferrihydrites or by the presence of occluded organic matter in addition to adsorbed organic matter in coprecipitates. Such a behavior was previously reported for the coprecipitation of lignin, but not for a forest floor extract (Eusterhues et al., 2011).

Three samples of each adsorption and the coprecipitation series were selected for the reduction experiments (Table 1).

FTIR-spectra of adsorbed and coprecipitated organic matter differ from the original forest floor extract. The peak assigned to C=O in protonated carboxyl groups (1723 cm^{-1}) is reduced to merely a shoulder (seen only in the 2nd derivative of AFhD and CFhD at 1716 and 1712 cm^{-1}), while the signal related to deprotonated carboxyl groups (1622 cm^{-1} in FFE) is increased and shifted to higher wavenumbers (1632, 1631 cm^{-1}). This pattern is explained by the formation of inner-sphere surface complexes between carboxylic acids and Fe oxides surfaces or dissolved metals (Kang et al., 2008; Persson and Axe, 2005). The peak at 1148 cm^{-1} (C-O in carbohydrates) in the forest floor extract is not visible in the adsorbed or coprecipitated organic matter and the peak at 1089 cm^{-1} is slightly shifted to lower wavenumbers (1082, 1079 cm^{-1}). Both changes point to a fractionation of carbohydrates during adsorption or coprecipitation. The absence of the sharp peaks at 1384 and 825 cm^{-1} shows that coprecipitates and adsorption complexes are free of nitrate. We assume, the adsorption of organic matter has removed the surface bound nitrate, which could not be removed from ferrihydrite through washing (Fh in Figure 2), and the natural nitrate from the forest floor extract did not react with the Fe oxides (FFE in Figure 2).

FTIR spectra and their second derivatives of adsorbed and coprecipitated organic matter are remarkably similar. Small differences however exists for the main carbohydrate peak and its shoulders, but seem mainly related to the amount of mineral-bound organic matter: While carbohydrates are represented by peaks at ~1125 and ~1080 and ~1040 cm^{-1} in samples with small C concentrations (AFhA; CFhA), samples with large C concentration show a strong peak at ~1080 cm^{-1} and a shoulder at ~1040 cm^{-1} (AFhD, AFhB, CFhD).

The highly surface-sensitive XPS technique provides the chemical composition of typically less than 10 nm of the sample surface (Seah and Dench, 1979).). High resolution XPS spectra of the C1s, N1s, Fe2p, and P2p lines are given in Figure 4. Weak S2p signals (data not shown) above the detection limit were found for the forest floor extract and for coprecipitates and adsorption complexes with low C concentrations (< 115 mg/g). The absence of S in complexes with higher organic matter contents may imply that adsorption of the forest floor organic material outcompetes adsorption of sulfate. The N1s and the P2p peaks show considerable noise (Figure 4), which leads to large scatter for C/N and C/P ratios (Figure 5). Nevertheless, the data show that the C/N ratio and the C/P ratio of coprecipitates and adsorption complexes are clearly higher than that of the original forest floor extract. While C/P-ratios for the coprecipitated organic matter are very similar to that of the adsorbed organic matter, a slightly, but significantly higher mean C/N-ratio (40) for the adsorbed

organic matter is observed in comparison to a C/N of 35 for coprecipitated organic matter (α = 0.05; T-test). The C1s peak can be deconvoluted into four peaks as shown exemplary for the forest floor extract (Figure 4) and assigned to 285.0 eV: C-C and C-H; 286.6 eV: C-O and C-N; 288.2 eV: C=O and N-C=O, and 289.3 eV: O-C=O (Arnarson and Keil, 2001). The adsorbed and coprecipitated organic matter was found enriched in aliphatic C (C-C, C-H) and carboxylic C (O-C=O), but compositional differences between adsorbed and coprecipitated cannot be seen (data not shown).

To find out whether the exposed ferrihydrite surface differs between coprecipitated ferrihydrites and ferrihydrites with adsorbed organic matter, we determined the C/Fe-ratio (Figure 5A). Although coprecipitated ferrihydrites might have occluded a major part of the associated organic matter inside their aggregates, the XPS C/Fe-ratio was found to be similar for samples with the same C concentration. We therefore assume that the accessibility of the ferrihydrite surface for reducing agents or microbial cells is not systematically different in coprecipitates and in ferrihydrites with adsorbed organic matter.

3.2 Microbial Fe(III) reduction by *Geobacter bremensis*

Incubation of ferrihydrite-organic matter associations with *G. bremensis* (Figure 6) revealed that reaction rates and degree of reduction varied with the amount of mineral associated organic matter: Increasing organic matter-loadings on ferrihydrite led to decreasing initial reaction rates and a decreasing degree of reduction for ferrihydrites with coprecipitated as well as adsorbed organic matter (Table 1). Also, samples of the coprecipitation series were more reactive than samples of the adsorption series, when comparing samples with similar organic matter contents. In case of AFhA, the sample with the smallest amount of adsorbed organic matter (44 mg g^{-1} C), the initial reaction rate was smaller (0.0017 min^{-1}) than that of the organic matter-free control ferrihydrite Fh (0.0020 min^{-1}) while the degree of dissolution at day 17 was similar (64%) to that of the control ferrihydrite (63%). In case of CFhA, the ferrihydrite sample with the smallest amount of coprecipitated organic matter (44 mg g^{-1} C), initial reaction rate (0.0021 min^{-1}) and degree of dissolution (82%) were even larger than for the control ferrihydrite Fh.

We conclude that the mineral-bound organic matter results in a surface passivation of the ferrihydrite surface. The fact that coprecipitates were more easily reduced than ferrihydrites with adsorbed organic matter may be explained by smaller and more defective individual ferrihydrite crystals in coprecipitates (Eusterhues et al., 2008) and a therefore larger specific

surface area. A possibly larger accessible outer ferrihydrite surface in coprecipitates compared to ferrihydrite with the same amount of adsorbed organic matter can be ruled out based on XPS results (Figure 5A). We assume that these effects dominate over the surface passivation effect due to associated organic matter in case of the fast and extensive reduction of CFhA. A systematically different aggregate structure between ferrihydrite with adsorbed organic matter and coprecipitated ferrihydrites may also have influenced the availability of the mineral surface (Pédrot et al., 2011). A possibly different composition of the mineral-bound organic matter in coprecipitates compared to adsorption complexes is a further aspect, which has to be taken into account. Although FTIR spectra and XPS spectra were very similar, we cannot exclude differences between adsorbed and coprecipitated material. In a previous experiment with a distinct forest floor extract (Eusterhues et al., 2011) FTIR spectra had also been very similar, whereas ^{13}C NMR analyses of the non-reacted fraction had shown that the adsorbed organic matter was enriched in O-alkyl C (carbohydrates), but depleted in carbonyl C and alkyl C relative to the coprecipitated material. (It was not possible to obtain NMR spectra of reasonable quality of the material used in this study. Formation of soluble Fe complexes in the supernatant might be an explanation.) However, this knowledge does not help us to judge the possibly different efficiency with which the possibly different fractions may inhibit ferrihydrite reduction. The ability of molecules to form bi- or multinuclear inner-sphere bonds was recognized to make strong inhibitors with respect to mineral dissolution (Stumm, 1997), while the presence of electron accepting and electron donating groups in the organic material controls its ability to act as an electron shuttle and promote reduction. Quinones and condensed aromatic groups have been shown to be redox active in humic acids and chars (Dunnivant et al., 1992; Scott et al., 1998; Klüpfel et al., 2014). While we do not expect any condensed aromatics, we cannot quantify quinones or multinuclear inner-sphere bonds in the mineral-bound organic matter.

Our microbial reduction results are surprisingly different from experiments performed by Shimizu et al., (2013), who coprecipitated ferrihydrite with standard humic acids and monitored reduction by *Shewanella putrefaciens* strain CN-32. They found that increasing amounts of coprecipitated humic acid led to elevated microbial reduction. At high humic acid loadings (C/Fe = 4.3) reduction rates based on dissolved Fe(II) were faster than that of pure ferrihydrite, whereas lower humic acid loadings (C/Fe < 1.8) resulted in slower reduction rates. Pure ferrihydrite was reduced at medium reduction rates. The experiments of Shimizu et al., (2013) are in accordance with the overall assumption that the coprecipitated humic acid are used by *Shewanella* to transfer electrons from the cell to the Fe oxide and advance its

363 electron shuttling process. A threshold amount of mineral-associated humic acid was assumed
364 to be necessary before electron shuttling accelerates ferrihydrite dissolution (Shimizu et al.,
365 2013).

366 However, the enhancement of electron shuttling might have been especially strong for the
367 experimental conditions chosen by Shimizu et al. (2013), because the content of aromatic
368 groups and quinones is usually much larger in humic acid than in forest floor extracts as used
369 in this study. Accordingly, Piepenbrock et al. (2014) could show that the electron accepting
370 capacity, i.e. the concentration of redox-active functional groups, of a natural forest floor
371 extract was only half as high as that of the Pahokee Peat Humic Acid.

372 By comparing the two studies, the question arises if differences in electron transfer
373 mechanisms applied by the δ-Proteobacteria *Geobacter* and the γ-Proteobacteria *Shewanella*
374 can explain whether mineral-bound organic matter increases or decreases the reducibility of
375 Fe oxides. In general, the following electron transfer strategies have been discussed in the
376 literature: i) direct electron transfer (DET) by either membrane-bound redox-enzymes (Nevin
377 and Lovley, 2000) or bacterial nanowires (Reguera, et al., 2005; Gorby et al., 2006;
378 Malvankar et al., 2011) and ii) mediated electron transfer (MET) using either chelators (Nevin
379 and Lovley, 2002; Kraemer, 2004) or redox shuttling compounds that are produced by the cell
380 itself (Marsili et al., 2008) or are abundant in the extracellular environment (Lovley et al.,
381 1996). *Geobacter* has been found to require direct contact to the mineral surface, but is also
382 discussed to use nanowires for electron transfer (Malvankar et al., 2012; Boesen and Nielsen,
383 2013). *Geobacte*r species can conserve energy from the transfer of electrons to a variety of
384 extracellular electron acceptors including metals like Mn(IV) and U(VI), but also electrodes
385 and humic acid. *Shewanella* is long known to not rely on direct contact (Arnold et al., 1990;
386 Caccavo et al., 1997; Lies et al., 2005) and to produce chelating compounds like flavins (von
387 Canstein, 2008). A study of Kotloski and Gralnick (2013) recently showed that flavin electron
388 shuttling but not direct electron transfer or nanowires is the primary mechanism of
389 extracellular electron transfer by *Shewanella oneidensis*.

390 For *Geobacter* increasing amounts of mineral-bound organic matter decreased reduction rates
391 and degree of reduction, probably because reactive surface sites of the mineral are blocked by
392 adsorbed organic matter molecules. Additionally, increasing amounts of organic matter will
393 increase the negative charge of the particle surface, which may also impede their accessibility
394 for negatively charged microbial cells (Shimizu et al., 2013 and ref. therein). For *Shewanella*
395 species, which use chelating agents and electron shuttles, smaller amounts of adsorbed

organic matter hinder reduction by passivation of reactive surface sites, whereas large amounts of mineral-bound organic matter can be used to enhance electron shuttling or chelating of Fe. Interestingly, we did not observe such an increase in reduction rates at very large organic matter loadings, although also *Geobacter* species are able to reduce extracellular organic matter. This can either be explained by the lower concentration of redox active groups in natural dissolved organic matter compared to humic acid (Piepenbrock et al., 2014) or by species-dependent different capabilities.

Partial reduction of Fe oxides during microbial reduction is explained by surface passivation through adsorption of Fe(II) (Roden and Urrutia, 1999, Liu et al., 2001). Similar to Shimizu et al. (2013) our study shows that mineral-bound organic matter has to be taken into account as an additional control of Fe(III) reduction. Because dissolved organic matter is present in almost all natural environments such as lakes, wetlands and soils, the occurrence of mineral-bound organic matter on Fe oxides is more likely than that of pure Fe oxides surfaces. Since the precipitation of ferrihydrite usually takes place from organic matter-containing solutions, the occurrence of coprecipitates is also more likely than that of ferrihydrite with only adsorbed organic matter. For these coprecipitates, a smaller crystal size and a more defective structure must be considered to result in faster reaction rates than compared to ferrihydrites with similar amounts of adsorbed organic matter.

Geobacteraceae have been studied intensively and are thought to contribute significantly to Fe(III)-reduction in most soils and sediments (Lovley, 2011 and ref. therein). Therefore we believe the findings of this study might contribute to a better understanding of processes occurring in a wide variety of environments.

3.3 Mineral transformation during microbial reduction

Investigating the solid remnants after 52 days of microbial reduction revealed that the formation of secondary minerals has been affected by the presence of mineral-bound organic matter (Table 2). Besides salts, such as halite, sal ammoniac and nahcolite, originating from the medium, we detected the neo-formation of goethite (FeOOH) and siderite ($FeCO_3$). Siderite was found after reduction of pure ferrihydrite (Fh) and in samples with rather low amounts of organic matter (AFhA, CFhA, CFhB), goethite was only found after reduction of the pure ferrihydrite. Thus, the formation of siderite was limited to experiments with high reduction rates and high degrees of reduction, where the solubility product of siderite was likely exceeded. The formation of goethite only took place in the absence of organic matter.

This is in accordance with the general observation that goethite formation is hindered by organic matter (Schwertmann, 1966; Schwertmann, 1970) and with the experiments by Henneberry et al. (2012), who reduced ferrihydrite-organic matter coprecipitates by S(-II) and Fe(II) and observed no mineral transformation as well. Shimizu et al. (2013) also found goethite only in the control experiments with pure ferrihydrite, whereas the reduction of ferrihydrite-organic matter association favored the formation of green rust and magnetite.

Goethite formation during reduction is assumed to be catalyzed by Fe(II) ions which adsorb to the Fe oxide surface (Hansel et al., 2003; Thompson et al., 2006; Yee et al., 2006). We expected a competition of Fe(II) with organic matter and therefore a decreased amount of goethite formation in our experiments. However, this does not explain that no goethite was formed during the reduction of ferrihydrite in presence of only a small amount of mineral-bound organic matter. Possible explanations could be the detection limit of XRD (~5%) and a full coverage of Fe(II)-reactive sites on ferrihydrite (Shimizu et al., 2013). Furthermore, a preferential reaction of Fe(II) with the mineral-bound organic matter instead of the Fe oxide surface could be considered.

3.4 Abiotic Reduction by Na-Dithionite

During abiotic reduction with Na-dithionite (Figure 7, Table 1) we observed highest initial reduction rates for the pure ferrihydrite and systematically decreasing reduction rates with increasing amounts of mineral-bound organic matter. Likewise, the degree of reduction after 75 min was generally decreasing with increasing organic matter. An exception is sample CFhA, for which the dissolved Fe(II) was estimated to be larger than the total Fe, which is not possible. Therefore we did not calculate reduction rate and degree of reduction for this sample. Reduction rates and the degree of reduction again tend to be larger for coprecipitated ferrihydrite. Thus, abiotic reduction experiments displayed the same overall picture of the reactivity of the ferrihydrite-organic matter associations as the microbial reduction experiments with *G. bremensis*. However, reduction rates for Na-dithionite are two to three orders of magnitude larger.

The data for abiotic reduction could be well represented by the model by Christoffersen and Christoffersen (1976; Table 1). It is interesting to note that γ the parameter describing particle shape, particle size, reactive site density and particle heterogeneity in this model is increasing with increasing amounts of mineral-bound organic matter from 1.3 to 2.6 for coprecipitates and from 2.9 to 7.4 for ferrihydrites with adsorbed organic matter (Table 1). Reduction of

462 pure ferrihydrite gave a γ of 2.4. The theoretical value for ideally dissolving isotropic particles
463 is 2/3. Houben (2003) found a γ of 1.5 for reduction of ferrihydrite with Na-dithionite; Larsen
464 et al. (2006) reported values between 1 and 2.2 for reduction of aquifer material by ascorbic
465 acid. Roden (2004) observed a γ of 0.7 for synthetic ferrihydrite reduced by ascorbic acid and
466 values between 0.8 and 1.8 for natural Fe oxides. Reducing the same material microbially by
467 *Shewanella* led to much higher values of γ of 5.8 to 11.8. Likewise he observed lower degrees
468 of reduction for microbial reduction than for reduction by ascorbic acid. He concluded that the
469 low degrees of reduction as well as the high values for γ during microbial reduction reflect
470 "the inhibitory effect of Fe(II) accumulation on enzymatic electron transfer" (Roden, 2004).
471 However, because we observed high γ values for abiotic reduction (Table 1), we propose that
472 surface passivation by organic matter leads to a high γ, also.
473

474 ## 3.5 Summary and environmental implications

475 In the present study mineral-bound soil organic matter has been shown to decrease microbial
476 reduction by *G. bremensis* and abiotic reduction by Na-dithionite of ferrihydrite. The
477 reactivity of ferrihydrites with adsorbed organic matter differed from ferrihydrites
478 coprecipitated with organic matter: at similar organic matter contents higher initial reaction
479 rates and higher degrees of reduction were observed for coprecipitated ferrihydrites. Their
480 higher reactivity can be explained by the smaller crystal size and higher number of crystal
481 defects due to poisoning of crystal growth in the presence of organic matter during
482 coprecipitation. However, other aspects such as a different composition of the associated
483 organic matter and/or a different aggregate structure may also influence reduction kinetics. At
484 low concentrations of coprecipitated organic matter these effects may be stronger than the
485 surface passivation by the mineral-bound organic matter and lead to an even faster reduction
486 of coprecipitates than of pure ferrihydrite. We therefore propose that, in addition to the
487 accumulation of Fe(II), the organic matter coverage of Fe oxide surfaces is discussed as a
488 further widespread mechanism to slow down or cease enzymatic reduction.

489 The secondary formation of Fe minerals resulting from microbial reduction was also
490 influenced by the amount of mineral-bound organic matter. Goethite was only found after
491 reduction of the organic matter-free ferrihydrite and siderite was only detected when
492 ferrihydrites with relatively low amounts of mineral-bound organic matter were reduced. For
493 e.g. soils, where we assume that an organic matter covered Fe oxide surface is rather the rule
494 than the exception, we conclude that goethite and siderite formation is less likely than in
495 typical microbial reduction experiments. Growth of new minerals will influence the cycling of

Fe as well as of the usually associated nutrients and contaminants, because both goethite and siderite represent thermodynamically more stable sinks for the fixation of Fe(III) and Fe(II) than ferrihydrite and have different mineral surfaces.

Comparison to the studies of Pédrot et al. (2011) and Shimizu et al. (2013) let us assume that the electron transfer mechanism of a microorganism controls whether or not mineral-bound organic matter decreases or increases microbial reduction. Whereas *Shewanella* may use own redox-active products to enhance electron shuttling, direct contact requiring *Geobacter* may not be able to reach the oxide surface when blocked by organic matter. If this hypothesis holds true, in natural environments, the likely presence of mineral-bound organic matter on Fe oxide surfaces may increase or decrease Fe reduction, depending on the dominating types of microorganisms. On the other hand, the composition or activity of the Fe reducing microbial community might be regulated by the mean coverage of the Fe oxide surfaces. Systems with low dissolved organic matter concentrations and low organic matter loadings on Fe oxides might be favored by microorganisms requiring direct contact for reduction such as *Geobacter*, whereas systems with high dissolved organic matter concentrations might be ideal for electron shuttle or ligand driven microbial reduction.

4 Conclusions

Fe oxides are recognized as very important mineral phases, which stabilize their mineral-bound organic matter against microbial degradation in the long-term. In redoximorphic soils, it will depend on the type of reducing microorganism whether the presence of mineral-bound organic matter will inhibit dissolution of the carrier mineral and support organic matter storage at the same time. When direct electron transfer is the main mechanism for microbial Fe(III) reduction, the organic matter coverage will protect the underlying Fe mineral and promote its own preservation, whereas the opposite must be assumed for soils dominated by microorganisms using electron shuttles or ligands for Fe(III) reduction.

Acknowledgements

525 Part of this work was financially supported by the priority program SPP 1315
526 “Biogeochemical Interfaces in Soil” of the Deutsche Forschungsgemeinschaft (DFG). Many
527 thanks to Angelika Kölbl, Markus Steffens and Ingrid Kögel-Knabner (Lehrstuhl für
528 Bodenkunde, Technische Universität München) for NMR-data and to Ralf Wagner (Chair of
529 Materials Science, University of Jena) for XPS measurements. We also highly appreciate help
530 in the laboratory by Katy Pfeiffer, Gundula Rudolph and Christine Götze.

References

Abdulla, H. A. N., Minor, E. C., Dias, R. F., and Hatcher, P. G.: Changes in the compound classes of dissolved organic matter along an estuarine transect: A study using FTIR and C-13 NMR, Geochimica et Cosmochimica Acta, 74, 3815-3838, 2010.

Amstaetter, K., Borch, T., and Kappler, A.: Influence of humic acid imposed changes of ferrihydrite aggregation on microbial Fe(III) reduction, Geochimica et Cosmochimica Acta, 85, 326-341, 2012.

Arnarson, T. S. and Keil, R. G.: Organic-mineral interactions in marine sediments studied using density fractionation and X-ray photoelectron spectroscopy, Organic Geochemistry, 32, 1401-1415, 2001.

Arnold, R. G., Hoffmann, M. R., Dichristina, T. J., and Picardal, F. W.: Regulation of Dissimilatory Fe(III) Reduction Activity in Shewanella-Putrefaciens, Applied and Environmental Microbiology, 56, 2811-2817, 1990.

Bigham, J. M., Fitzpatrick, R. W., and Schulze, D. G.: Iron oxides. In: Soil mineralogy with environmental applications, Dixon, J. B. and Schulze, D. G. (Eds.), SSSA Book Ser. No. 7, Soil Science Society of America, Madison, WI, 2002.

Boesen, T. and Nielsen, L. P.: Molecular Dissection of Bacterial Nanowires, Mbio, 4, 2013.

Caccavo, F., Schamberger, P. C., Keiding, K., and Nielsen, P. H.: Role of hydrophobicity in adhesion of the dissimilatory Fe(III)-reducing bacterium Shewanella alga to amorphous Fe(III) oxide, Applied and Environmental Microbiology, 63, 3837-3843, 1997.

Christoffersen, J. and Christoffersen, M. R.: Kinetics of dissolution of calcium-sulfate-dihydrate in water Journal of Crystal Growth, 35, 79-88, 1976.

Cismasu, A. C., Michel, F. M., Tcaciuc, A. P., Tyliszczak, T., and Brown, J., G.E.: Composition and structural aspects of naturally occurring ferrihydrite, Comptes Rendus Geoscience, 343, 210-218, 2011.

Cornell, R. M. and Schwertmann, U.: The Iron Oxides: Structure, Properties, Reactions, Occurrences and Uses, Wiley-VCH Verlagsgesellschaft, Weinheim, 2003.

Dunnivant, F. M., Schwarzenbach, R. P., and Macalady, D. L.: Reduction of substituted nitrobenzenes in aqueous-solution containing natural organic matter, Environmental Science & Technology, 26, 2133-2141, 1992.

Ebadi, A., Mohammadzadeh, J. S. S., and Khudiev, A.: What is the correct form of BET isotherm for modeling liquid phase adsorption? Adsorption-Journal of the International Adsorption Society, 15, 65-73, 2009.

565 Eusterhues, K., Neidhardt, J., Hädrich, A., Küsel, K., and Totsche, K. U.: Biodegradation of
566 ferrihydrite-associated organic matter, Biogeochemistry, DOI 10.1007/s10533-013-9943-0,
567 2014.
568 Eusterhues, K., Rennert, T., Knicker, H., Kögel-Knabner, I., Totsche, K. U., and
569 Schwertmann, U.: Fractionation of Organic Matter Due to Reaction with Ferrihydrite:
570 Coprecipitation versus Adsorption, Environmental Science & Technology, 45, 527-533,
571 2011.
572 Eusterhues, K., Rumpel, C., and Kögel-Knabner, I.: Organo-mineral associations in sandy
573 acid forest soils: importance of specific surface area, iron oxides and micropores, European
574 Journal of Soil Science, 56, 753-763, 2005.
575 Eusterhues, K., Wagner, F. E., Häusler, W., Hanzlik, M., Knicker, H., Totsche, K. U., Kögel-
576 Knabner, I., and Schwertmann, U.: Characterization of Ferrihydrite-Soil Organic Matter
577 Coprecipitates by X-ray Diffraction and Mössbauer Spectroscopy, Environmental Science
578 & Technology, 42, 7891-7897, 2008.
579 Gorby, Y. A., Yanina, S., McLean, J. S., Rosso, K. M., Moyles, D., Dohnalkova, A.,
580 Beveridge, T. J., Chang, I. S., Kim, B. H., Kim, K. S., Culley, D. E., Reed, S. B., Romine,
581 M. F., Saffarini, D. A., Hill, E. A., Shi, L., Elias, D. A., Kennedy, D. W., Pinchuk, G.,
582 Watanabe, K., Ishii, S. i., Logan, B., Nealson, K. H., and Fredrickson, J. K.: Electrically
583 conductive bacterial nanowires produced by Shewanella oneidensis strain MR-1 and other
584 microorganisms, Proceedings of the National Academy of Sciences of the United States of
585 America, 103, 11358-11363, 2006.
586 Grosvenor, A. P., Kobe, B. A., Biesinger, M. C., and McIntyre, N. S.: Investigation of
587 multiplet splitting of Fe 2p XPS spectra and bonding in iron compounds, Surface and
588 Interface Analysis, 36, 1564-1574, 2004.
589 Hansel, C. M., Benner, S. G., Neiss, J., Dohnalkova, A., Kukkadapu, R. K., and Fendorf, S.:
590 Secondary mineralization pathways induced by dissimilatory iron reduction of ferrihydrite
591 under advective flow, Geochimica et Cosmochimica Acta, 67, 2977-2992, 2003.
592 Hansel, C. M., Benner, S. G., Nico, P., and Fendorf, S.: Structural constraints of ferric
593 (hydr)oxides on dissimilatory iron reduction and the fate of Fe(II), Geochimica et
594 Cosmochimica Acta, 68, 3217-3229, 2004.
595 Henneberry, Y. K., Kraus, T. E. C., Nico, P. S., and Horwath, W. R.: Structural stability of
596 coprecipitated natural organic matter and ferric iron under reducing conditions, Organic
597 Geochemistry, 48, 81-89, 2012.

598 Houben, G. J.: Iron oxide incrustations in wells. Part 2: chemical dissolution and modeling,
599 Applied Geochemistry, 18, 941-954, 2003.
600 Jambor, J. L. and Dutrizac, J. E.: Occurrence and constitution of natural and synthetic
601 ferrihydrite, a widespread iron oxyhydroxide, Chemical Reviews, 98, 2549-2585, 1998.
602 Jiang, J. and Kappler, A.: Kinetics of microbial and chemical reduction of humic substances:
603 Implications for electron shuttling, Environmental Science & Technology, 42, 3563-3569,
604 2008.
605 Jones, A. M., Collins, R. N., Rose, J., and Waite, T. D.: The effect of silica and natural
606 organic matter on the Fe(II)-catalysed transformation and reactivity of Fe(III) minerals,
607 Geochimica et Cosmochimica Acta, 73, 4409-4422, 2009.
608 Kang, S. H., Amarasiriwardena, D., and Xing, B. S.: Effect of dehydration on dicarboxylic
609 acid coordination at goethite/water interface, Colloid Surf. A-Physicochem. Eng. Asp.,
610 318, 275-284, 2008.
611 Kaiser, K., Mikutta, R., and Guggenberger, G.: Increased stability of organic matter sorbed to
612 ferrihydrite and goethite on aging, Soil Science Society of America Journal, 71, 711-719,
613 2007.
614 Kaiser, K. and Zech, W.: Dissolved organic matter sorption by mineral constituents of subsoil
615 clay fractions, Journal of Plant Nutrition and Soil Science, 163, 531-535, 2000.
616 Karltun, E., Bain, D. C., Gustafsson, J. P., Mannerkoski, H., Murad, E., Wagner, U., Fraser,
617 A. R., McHardy, W. J., and Starr, M.: Surface reactivity of poorly-ordered minerals in
618 podzol B horizons, Geoderma, 94, 265-288, 2000.
619 Klüpfel, L., Keiluweit, M., Kleber, M., and Sander, M.: Redox Properties of Plant Biomass-
620 Derived Black Carbon (Biochar), Environmental Science & Technology, 48, 5601-5611,
621 2014.
622 Kotloski, N. J. and Gralnick, J. A.: Flavin Electron Shuttles Dominate Extracellular Electron
623 Transfer by Shewanella oneidensis, Mbio, 4, 2013.
624 Kraemer, S. M.: Iron oxide dissolution and solubility in the presence of siderophores, Aquatic
625 Sciences, 66, 3-18, 2004.
626 Larsen, O. and Postma, D.: Kinetics of reductive bulk dissolution of lepidocrocite,
627 ferrihydrite, and goethite, Geochimica et Cosmochimica Acta, 65, 1367-1379, 2001.
628 Larsen, O., Postma, D., and Jakobsen, R.: The reactivity of iron oxides towards reductive
629 dissolution with ascorbic acid in a shallow sandy aquifer - (Romo, Denmark), Geochimica
630 et Cosmochimica Acta, 70, 4827-4835, 2006.

631 Lies, D. P., Hernandez, M. E., Kappler, A., Mielke, R. E., Gralnick, J. A., and Newman, D.
632 K.: Shewanella oneidensis MR-1 uses overlapping pathways for iron reduction at a
633 distance and by direct contact under conditions relevant for biofilms, Applied and
634 Environmental Microbiology, 71, 4414-4426, 2005.
635 Liu, C. X., Kota, S., Zachara, J. M., Fredrickson, J. K., and Brinkman, C. K.: Kinetic analysis
636 of the bacterial reduction of goethite, Environmental Science & Technology, 35, 2482-
637 2490, 2001.
638 Lovley, D. R., Coates, J. D., BluntHarris, E. L., Phillips, E. J. P., and Woodward, J. C.:
639 Humic substances as electron acceptors for microbial respiration, Nature, 382, 445-448,
640 1996.
641 Lovley, D. R., Ueki, T., Zhang, T., Malvankar, N. S., Shrestha, P. M., Flanagan, K. A.,
642 Aklujkar, M., Butler, J. E., Giloteaux, L., Rotaru, A.-E., Holmes, D. E., Franks, A. E.,
643 Orellana, R., Risso, C., and Nevin, K. P.: Geobacter: The Microbe Electric's Physiology,
644 Ecology, and Practical Applications. In: Advances in Microbial Physiology, Vol 59, Poole,
645 R. K. (Ed.), Advances in Microbial Physiology, 2011.
646 Malvankar, N. S., Tuominen, M. T., and Lovley, D. R.: Comment on "On electrical
647 conductivity of microbial nanowires and biofilms" by S. M. Strycharz-Glaven, R. M.
648 Snider, A. Guiseppi-Elie and L. M. Tender, Energy Environ. Sci., 2011, 4, 4366, Energy &
649 Environmental Science, 5, 6247-6249, 2012.
650 Malvankar, N. S., Vargas, M., Nevin, K. P., Franks, A. E., Leang, C., Kim, B.-C., Inoue, K.,
651 Mester, T., Covalla, S. F., Johnson, J. P., Rotello, V. M., Tuominen, M. T., and Lovley, D.
652 R.: Tunable metallic-like conductivity in microbial nanowire networks, Nature
653 Nanotechnology, 6, 573-579, 2011.
654 Marsili, E., Baron, D. B., Shikhare, I. D., Coursolle, D., Gralnick, J. A., and Bond, D. R.:
655 Shewanella secretes flavins that mediate extracellular electron transfer, Proceedings of the
656 National Academy of Sciences of the United States of America, 105, 3968-3973, 2008.
657 McIntyre, N. S. and Zetaruk, D. G.: X-Ray Photoeleectron Spectroscopic studies of iron
658 oxides, Analytical Chemistry, 49, 1521-1529, 1977.
659 Mikutta, C., Mikutta, R., Bonneville, S., Wagner, F., Voegelin, A., Christl, I., and
660 Kretzschmar, R.: Synthetic coprecipitates of exopolysaccharides and ferrihydrite. Part I:
661 Characterization, Geochimica et Cosmochimica Acta, 72, 1111-1127, 2008.
662 Nevin, K. P. and Lovley, D. R.: Lack of production of electron-shuttling compounds or
663 solubilization of Fe(III) during reduction of insoluble Fe(III) oxide by Geobacter
664 metallireducens, Applied and Environmental Microbiology, 66, 2248-2251, 2000.

Nevin, K. P. and Lovley, D. R.: Mechanisms for accessing insoluble Fe(III) oxide during dissimilatory Fe(III) reduction by Geothrix fermentans, Applied and Environmental Microbiology, 68, 2294-2299, 2002.

Pédrot, M., Le Boudec, A., Davranche, M., Dia, A., and Henin, O.: How does organic matter constrain the nature, size and availability of Fe nanoparticles for biological reduction? Journal of Colloid and Interface Science, 359, 75-85, 2011.

Persson, P. and Axe, K.: Adsorption of oxalate and malonate at the water-goethite interface: molecular surface speciation from IR spectroscopy, Geochimica et Cosmochimica Acta, 69, 541-552, 2005.

Piepenbrock, A., Schröder, C., and Kappler, A.: Electron Transfer from Humic Substances to Biogenic an Abiogenic Fe(III) Oxyhydroxide Minerals, Environmental Science & Technology, 48, 1656-1664, 2014.

Postma, D.: The reactivity of iron-oxides in sediments - A kinetic approach, Geochimica et Cosmochimica Acta, 57, 5027-5034, 1993.

Regelink, I. C., Weng, L., Koopmans, G. F., and Van Riemsdijk, W. H.: Asymmetric flow field-flow fractionation as a new approach to analyse iron-(hydr)oxide nanoparticles in soil extracts, Geoderma, 202, 134-141, 2013.

Reguera, G., McCarthy, K. D., Mehta, T., Nicoll, J. S., Tuominen, M. T., and Lovley, D. R.: Extracellular electron transfer via microbial nanowires, Nature, 435, 1098-1101, 2005.

Roden, E. E.: Analysis of long-term bacterial vs. chemical Fe(III) oxide reduction kinetics, Geochimica et Cosmochimica Acta, 68, 3205-3216, 2004.

Roden, E. E. and Urrutia, M. M.: Ferrous iron removal promotes microbial reduction of crystalline iron(III) oxides, Environmental Science & Technology, 33, 2492-2492, 1999.

Roden, E. E., Kappler, A., Bauer, I., Jiang, J., Paul, A., Stoesser, R., Konishi, H., and Xu, H. F.: Extracellular electron transfer through microbial reduction of solid-phase humic substances, Nature Geoscience, 3, 417-421, 2010.

Royer, R. A., Burgos, W. D., Fisher, A. S., Jeon, B. H., Unz, R. F., and Dempsey, B. A.: Enhancement of hematite bioreduction by natural organic matter, Environmental Science & Technology, 36, 2897-2904, 2002.

Schwertmann, U.: Influence of various simple organic anions on formation of goethite and hematite from amorphous ferric hydroxide, Geoderma, 3, 207-&, 1970.

Schwertmann, U.: Inhibitory effect of soil organic matter on crystallization of amorphous ferric hydroxide, Nature, 212, 645-&, 1966.

Schwertmann, U., Wagner, F., and Knicker, H.: Ferrihydrite-humic associations: Magnetic hyperfine interactions, Soil Science Society of America Journal, 69, 1009-1015, 2005.

Scott, D. T., McKnight, D. M., Blunt-Harris, E. L., Kolesar, S. E., and Lovley, D. R.: Quinone moieties act as electron acceptors in the reduction of humic substances by humics-reducing microorganisms, Environmental Science & Technology, 32, 2984-2989, 1998.

Seah, M. P. and Dench, W. A.: Quantitative electron spectroscopy of surfaces: A standard data base for electron inelastic mean free paths in solids, Surface and Interface Analysis, 1, 2-11, 1979.

Shimizu, M., Zhou, J., Schroeder, C., Obst, M., Kappler, A., and Borch, T.: Dissimilatory reduction and transformation of ferrihydrite-humic acid coprecipitates, Environmental Science & Technology, 47, 13375-13384, 2013.

Straub, K. L., Hanzlik, M., and Buchholz-Cleven, B. E. E.: The use of biologically produced ferrihydrite for the isolation of novel iron-reducing bacteria, Systematic and Applied Microbiology, 21, 442-449, 1998.

Straub, K. L. and Buchholz-Cleven, B. E. E.: Geobacter bremensis sp nov and Geobacter pelophilus sp nov., two dissimilatory ferric-iron-reducing bacteria, International Journal of Systematic and Evolutionary Microbiology, 51, 1805-1808, 2001.

Stumm, W.: Reactivity at the mineral-water interface: Dissolution and inhibition, Colloids and Surfaces A- Physicochemical and Engineering Aspects, 120, 143-166, 1997.

Tamura, H., Goto, K., Yotsuyan.T, and Nagayama, M.: Spectrophotometric determination of iron(II) with 1,10-phenanthroline in presence of large amounts of iron(III), Talanta, 21, 314-318, 1974.

Thompson, A., Chadwick, O. A., Rancourt, D. G., and Chorover, J.: Iron-oxide crystallinity increases during soil redox oscillations, Geochimica et Cosmochimica Acta, 70, 1710-1727, 2006.

Tipping, E.: The Adsorption of Aquatic Humic Substances by Iron-Oxides, Geochimica et Cosmochimica Acta, 45, 191-199, 1981.

Torn, M. S., Trumbore, S. E., Chadwick, O. A., Vitousek, P. M., and Hendricks, D. M.: Mineral control of soil organic carbon storage and turnover, Nature, 389, 170-173, 1997.

von Canstein, H., Ogawa, J., Shimizu, S., and Lloyd, J. R.: Secretion of flavins by *Shewanella* species and their role in extracellular electron transfer, Applied and Environmental Microbiology, 74, 615-623, 2008.

van der Zee, C., Roberts, D. R., Rancourt, D. G., and Slomp, C. P.: Nanogoethite is the dominant reactive oxyhydroxide phase in lake and marine sediments, Geology, 31, 993-996, 2003.

Yee, N., Shaw, S., Benning, L. G., and Nguyen, T. H.: The rate of ferrihydrite transformation to goethite via the Fe(II) pathway, American Mineralogist, 91, 92-96, 2006.

739

740 Table 1. Carbon concentration and C/Fe ratios of ferrihydrite-organic matter associations and
741 results of microbial and abiotic reduction experiments. See text for abbreviations.

				Reduction by *Geobacter bremensis*			Reduction by Na-dithionite					
				linear fit			linear fit			C&C		
		C	C/Fe	k	r^2	degree of dissolution*	k	r^2	degree of dissolution**	k	γ	r^2
		mg/g	mol/mol	h^{-1}		%	h^{-1}		%	h^{-1}		
control	Fh	2	0.02	0.0020	0.961	63	5.29	0.998	83	5.79	2.4	0.989
adsorbed OM	AFhA	44	0.39	0.0017	0.955	64	1.59	0.895	62	2.26	2.9	0.990
	AFhB	105	1.04	0.0011	0.965	42	0.72	0.895	30	1.07	7.2	0.991
	AFhD	181	2.46	0.0010	0.939	36	0.67	0.811	24	0.60	7.4	0.979
coprecipitated OM	CFhA	44	0.41	0.0021	0.950	82	-***	-	-	-	-	-
	CFhB	98	1.06	0.0016	0.983	68	1.09	0.975	64	1.32	1.9	0.995
	CFhD	182	2.83	0.0014	0.948	41	0.18	0.975	20	0.21	2.6	0.996

* degree of dissolution at day 17
**degree of dissolution at 75 min.
*** Please note that for the reduction by Na-dithionite for sample CFhA the dissolved Fe(II) was estimated to be larger than the total Fe, which is not possible. Therefore we did not calculate reduction rate and degree of reduction for this sample

742

743

744

745 Table 2. Mineral identification by XRD after reduction by *G. bremensis*. Sal ammoniac
746 (NH_4Cl) is abbreviated by "sal", nahcolite ($NaHCO_3$) by "nahc".

		halite	sal	nahc	calcite	siderite	goethite
control	Fh	x	x	x	x	x	x
adsorbed OM	AFhA	x				x	
	AFhB	x	(x)*				
	AFhD	x	x				
coprecipitated OM	CFhA	x	x			x	
	CFhB	x	x	x		x	
	CFhD	x	x				

747 *(x) less than 3 peaks identified

748

Figure captions

Figure 1. ^{13}C Cross polarization magic angle spinning nuclear magnetic resonance spectrum (^{13}C CPMAS NMR) of the forest floor extract.

Figure 2. FTIR spectra of the control ferrihydrite (Fh), the original forest floor extract (FFE), the adsorption complexes (AFhD, AFhB, AFhA), and the coprecipitates (CFhD, CFhB, CFhA). Second derivatives are given for spectra of the forest floor extract and the two ferrihydrite-organic matter complexes with the highest C concentration. Refer to text for abbreviations.

Figure 3. Ferrihydrite-associated C (normalized to the specific surface area of 197 m^2 g^{-1} of the control ferrihydrite) vs. C in the equilibrium solution. The line represents a BET-isotherm.

Figure 4. Background corrected XPS spectra of the control ferrihydrite (Fe2p, red), the forest floor extract (C1s, N1s, P2p, blue) and the incubated coprecipitates and adsorption complexes. Refer to text for abbreviations.

Figure 5. Comparison of chemical surface composition expressed in XPS signal ratios (C/Fe, C/N, and C/P) and bulk C content of Fh-OM associations. Dashed and dotted lines in (B) encircle XPS data for adsorption complexes and coprecipitates, respectively, to guide the eye.

Figure 6. Microbial reduction of ferrihydrite and ferrihydrite-organic matter associations in *Geobacter bremensis* cultures. The Fe(II) production was normalized to the total initial amount of Fe in ferrihydrite. The Fe(II)/Fe(total) of the ferrihydrite control (red stars) at day 52 was much lower than at day 17 and therefore unexpectedly low, letting us assume that this was due to unintentional oxidation at the end of the experiment in this sample (further details see text). Error bars represent standard deviations of triplicate cultures.

777 Figure 7. Abiotic reduction with Na-dithionite: Fe(II) production (normalized to the total
778 initial Fe in ferrihydrite) versus time. Lines represent the model by Christoffersen and
779 Christoffersen (1976). Note that the dissolved Fe(II) was estimated to be larger than the total
780 Fe for sample CFhA, which is unreasonable.

781

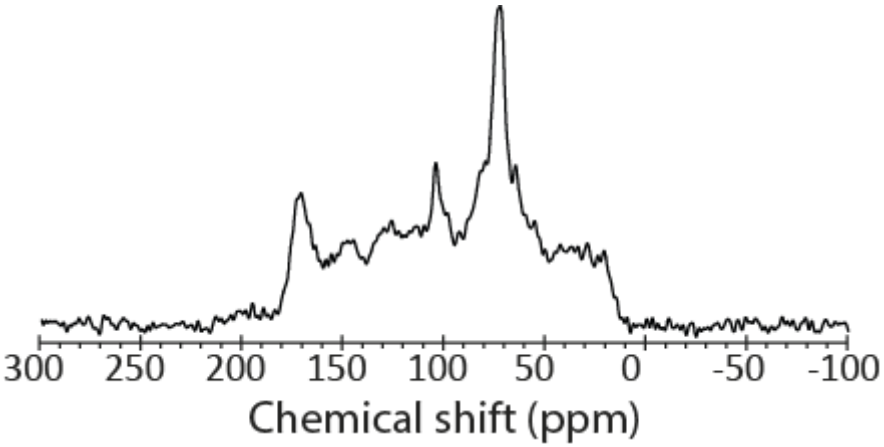

782

783

784 Figure 1. ^{13}C Cross polarization magic angle spinning nuclear magnetic resonance spectrum
785 (^{13}C CPMAS NMR) of the forest floor extract.

786

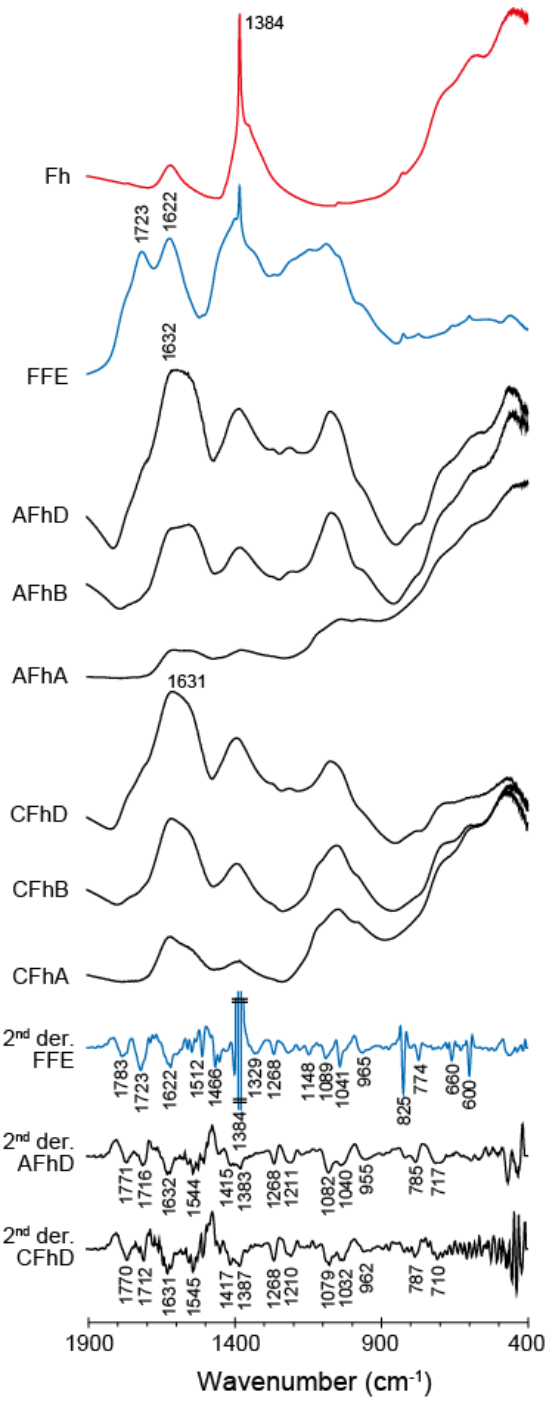

Figure 2. FTIR spectra of the control ferrihydrite (Fh), the original forest floor extract (FFE), the adsorption complexes (AFhD, AFhB, AFhA), and the coprecipitates (CFhD, CFhB, CFhA). Second derivatives are given for spectra of the forest floor extract and the two ferrihydrite-organic matter complexes with the highest C concentration. Refer to text for abbreviations.

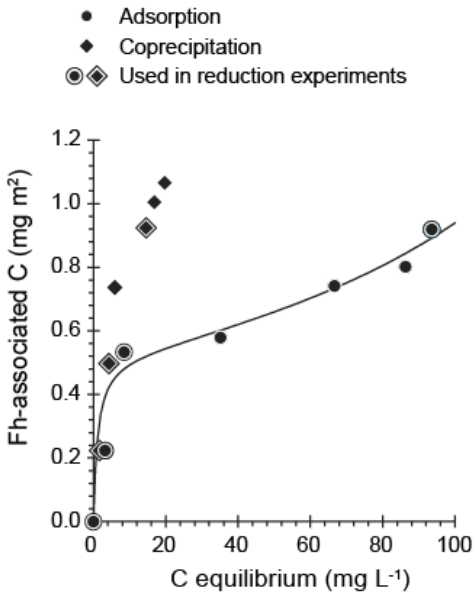

Figure 3. Ferrihydrite-associated C (normalized to the specific surface area of 197 m^2 g^{-1} of the control ferrihydrite) vs. C in the equilibrium solution. The line represents a BET-isotherm.

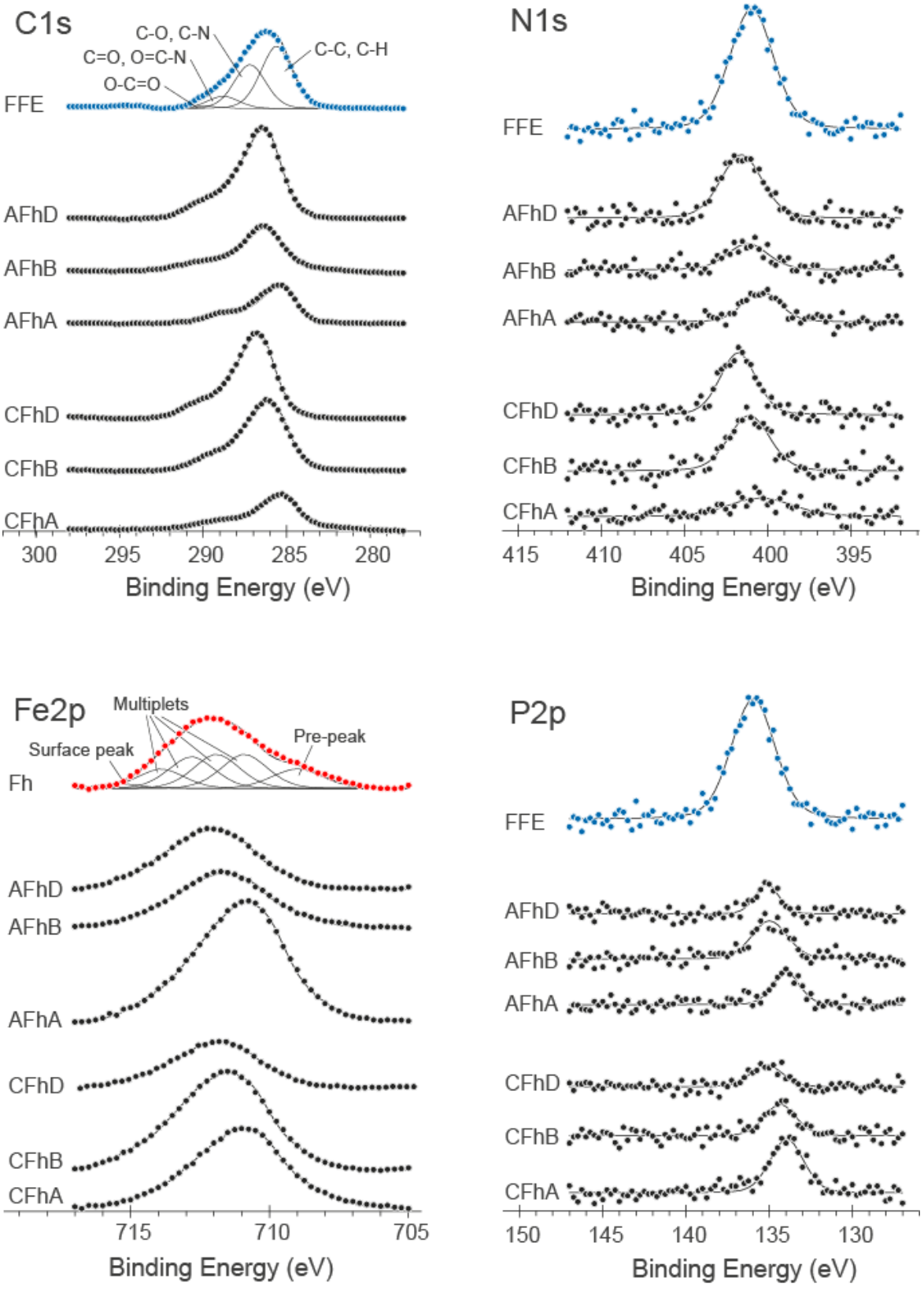

802

803 Figure 4. Background corrected XPS spectra of the control ferrihydrite Fh (only Fe2p, red),
804 the forest floor extract FFE (only C1s, N1s, P2p, blue) and the incubated coprecipitates
805 (CFhD, CFhB, CFhA) and adsorption complexes (AFhD, AFhB, AFhA). Refer to text for
806 abbreviations.

807

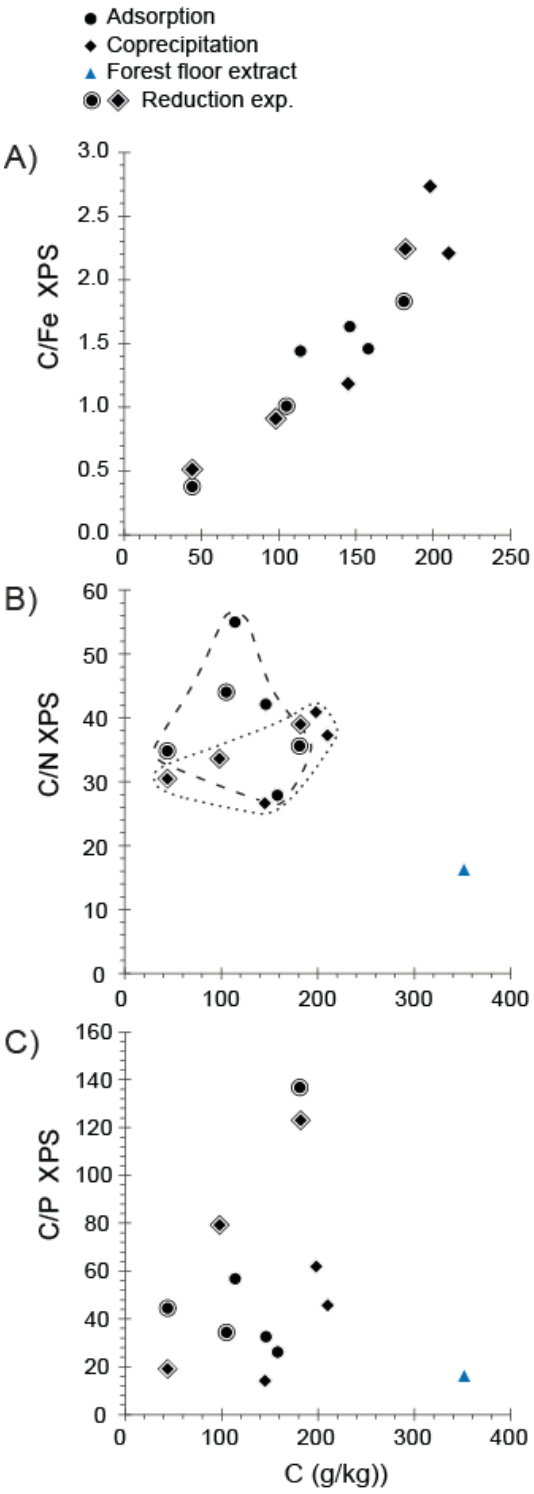

808

809 Figure 5. Comparison of chemical surface composition expressed in XPS intensity ratios
810 (C/Fe, C/N, and C/P) and bulk C content of Fh-OM associations. Dashed and dotted lines in
811 (B) encircle XPS data for adsorption complexes and coprecipitates, respectively, to guide the
812 eye.

813

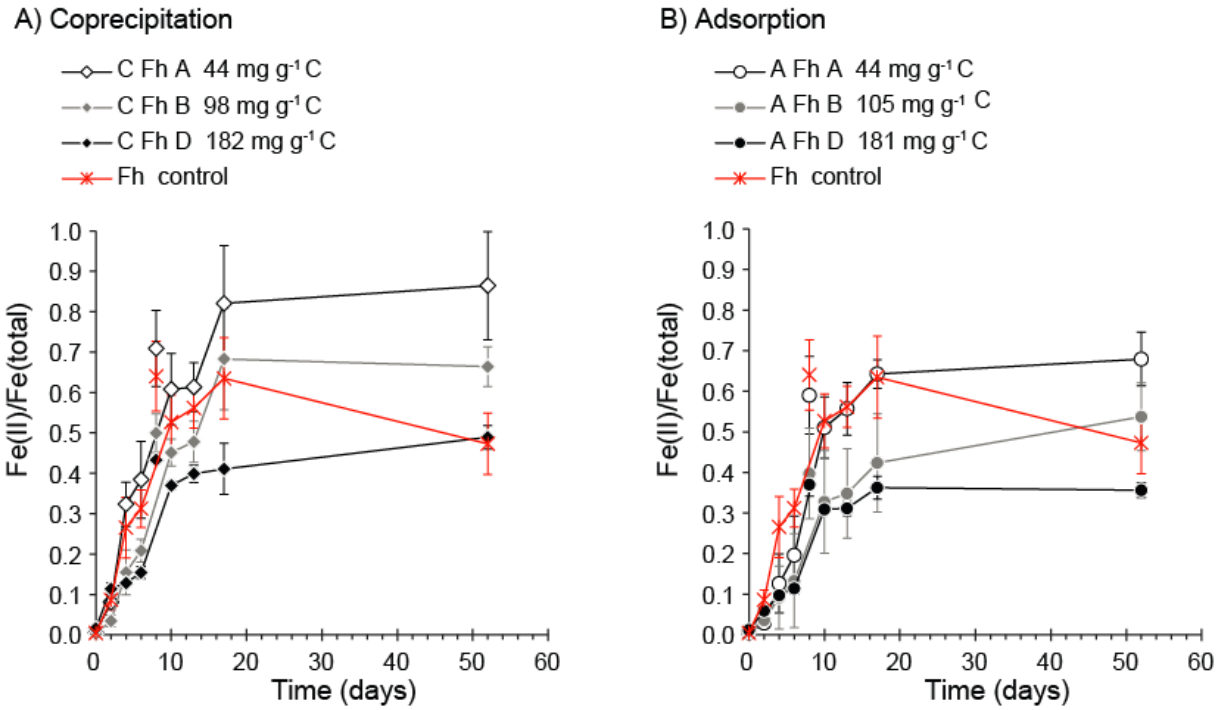

Figure 6. Microbial reduction of ferrihydrite and ferrihydrite-organic matter associations in *Geobacter bremensis* cultures. The Fe(II) production was normalized to the total initial amount of Fe in ferrihydrite. The Fe(II)/Fe(total) of the ferrihydrite control (red stars) at day 52 was much lower than at day 17 and therefore unexpectedly low, letting us assume that this was due to unintentional oxidation at the end of the experiment in this sample (further details see text). Error bars represent standard deviations of triplicate cultures.

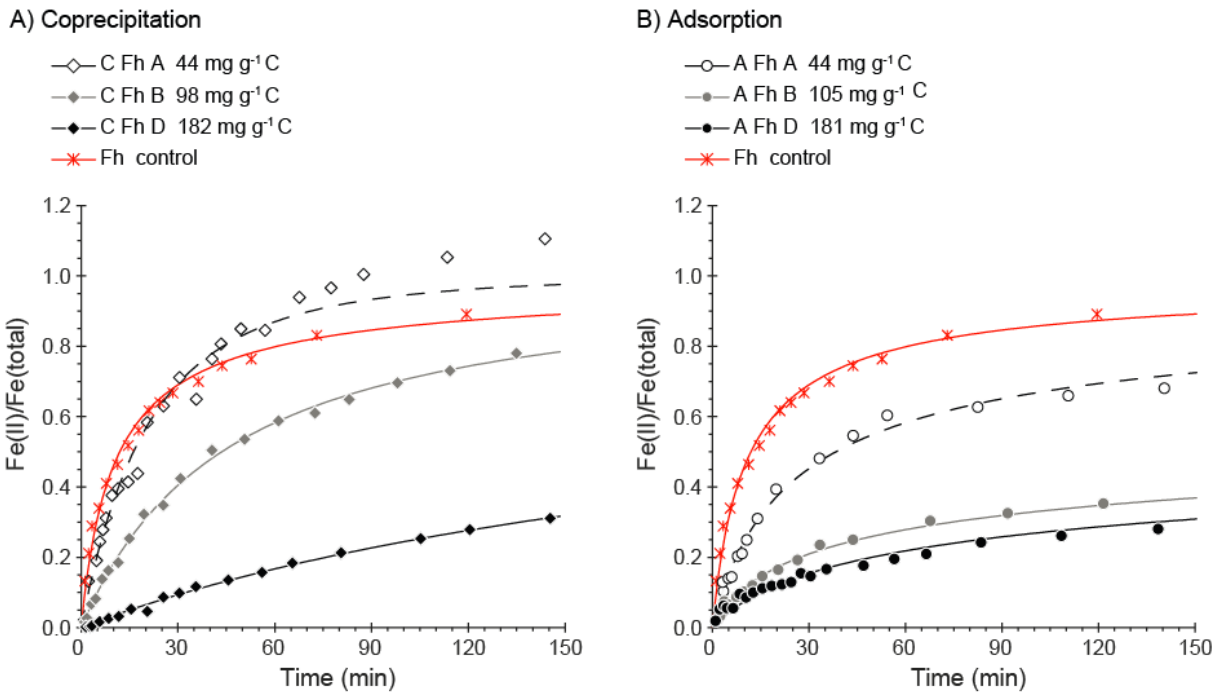

Figure 7. Abiotic reduction with Na-dithionite: Fe(II) production (normalized to the total initial Fe in ferrihydrite) versus time. Lines represent the model by Christoffersen and Christoffersen (1976). Note that the dissolved Fe(II) was estimated to be larger than the total Fe for sample CFhA, which is unreasonable (further details see text).